Heliyon 7 (2021) e08351

Contents lists available at ScienceDirect

Heliyon

journal homepage: www.cell.com/heliyon

Research article

Treatment of real industrial wastewater with high sulfate concentrations using modified Jordanian kaolin sorbent: batch and modelling studies

Banan Hudaib *

Chemical Engineering Department, Faculty of Engineering Technology, Al-Balqa Applied University, Amman 11134, Jordan

ARTICLE INFO

Keywords:
Wastewater
Sulfate ions
Kaolin
Batch
Equilibrium
Kinetics

ABSTRACT

In the present study, $BaCl_2$ modified Jordanian kaolin sorbent (obtained from Mahis, Jordan) was used to remove sulfate-contaminated industrial wastewater. The kaolin sample was pretreated to enhance its adsorption capacity and then characterized using X-Ray fluorescence (XRF) and Fourier Transform Infrared Spectroscopy (FTIR). Equilibrium isotherms for the adsorption parameters were carried out experimentally, and the adsorption data correlated very well with Freundlich and Temkin and Dubinin-Radushkevich models. Furthermore, the adsorption kinetics followed the pseudo-first-order and intraparticle diffusion models perfectly. The estimated value of the maximum adsorption capacity $q_m = 85.08$ mg/g indicates that kaolin has a very high capacity to adsorb sulfate ions at studied parameters. The estimated value of the mean free energy (4.87 kJ/mol) is very low, confirming physical type adsorption. The study results established that modified Jordanian kaolin could serve as a safe and effective natural adsorbent for sulfate-contaminated industrial wastewater.

1. Introductions

Jordan is classified as a semi-arid to arid country and considered among the world's poorest water resources availability (Saidan et al., 2020). Industries are considered the primary source of significant reusable effluents with production and demand of high amount of water, which bring forward the necessity for an economical process to reuse this pollutant discharged water. The reused water is vital in sustainable water resources management and is used in different applications, including agricultural irrigation, industrial processes, and others (Saidan et al., 2020).

Sulfate (SO_4^{2-}) is a significant primary ion present in natural water, municipal, and industrial wastewater (Tang et al., 2017). The primary sources of sulfate in natural water are chemical weathering and sulfur-containing minerals' oxidation processes (Akoh et al., 2020). Effluents discharged from many industries such as pharmaceutical wastewater, aluminum productions, printing, and dyeing have increased the concentration of sulfate in water over time (Tejada-Tovar et al., 2021).

It is often considered nontoxic, though high water sulfate concentrations will affect the balance of its natural cycle in the environment and can lead to human health implications with prolonged ingestion, scaling of pipes and public water supplies; when the concentration exceeds 600 mg L^{-1}, it can cause a laxative effect, dehydration, and gastric upset (Cao et al., 2011). Therefore, the sulfate ion needs to be removed from wastewater before it is discharged into the environment.

Many countries like Jordan set the industrial effluent range as 200–500 mg/L (Ministry of Water and Irrigation 2009). Hence, developing low-cost, sustainable treatment methods for removing sulfate is necessary to meet the industrial process demands and the environmental regulations. Removal of high sulfate concentration from wastewater can be achieved by several physicals, biological and chemical processes. These processes include electrocoagulation (Rodrigues et al., 2020), ion exchange (Tang et al., 2017), flotation (Amaral Filho et al., 2016), membrane filtration, and reverse osmosis (Al-Zoubi et al., 2007), chemical precipitation (Dhayabaran et al., 2017), and adsorption (Sadeghalvad et al., 2017). The adsorption method, either batch or continuous columns, is considered an effective treatment for removing sulfate for its simplicity, efficiency, and relatively low cost (Akoh et al., 2020).

Many non-conventional adsorbent materials have been tested for their adsorption capacity to remove pollutants (Al-Zoubi et al., 2020). However, The most promising material used as an alternative cheapest non-conventional adsorbents is clay minerals (Mustapha et al., 2019). Kaolinite is a layered silicate clay mineral that forms Kaolin's primary mineral component, a new promising potential adsorbent characterized by its high specific area, stability, structural characteristics, and

* Corresponding author.
E-mail address: banan.hudaib@bau.edu.jo.

https://doi.org/10.1016/j.heliyon.2021.e08351
Received 7 September 2021; Received in revised form 25 October 2021; Accepted 5 November 2021

availability (Mustapha et al., 2019). Kaolin's modification using inorganic and organic compounds is used to enhance its adsorption capacity and efficiency (Shaban et al., 2018; Diab et al., 2015).

Various adsorbents were used for the treatment of sulfate-contaminated wastewater. (Moret and Rubio 2003; Sadeghalvad et al., 2016) used Chitin-based shrimp shells as bio-sorbent for the removal of sulfate ions from mining liquid effluents. High sulfate adsorption [156 mg/g] was measured, which was explained by the excellent bond of amine and hydroxyl groups of chitin with sulfate. Cao et al. (2011) also studied using modified rice straw bio-sorbent for sulfate removal from an aqueous solution. The results showed that modified straw shows a higher sulfate maximum adsorption capacity (74.76 mg/g) than raw straw (11.68 mg/g). Mulinari and da Silva (2008) investigated a modified sugarcane bagasse cellulose with zirconium oxychloride (Cell/ZrO$_2$.nH2O) for adsorption of sulfate ions in an aqueous solution. The results demonstrated that the adsorption capacity was about 28 mg/g for sulfate ions. Runtti et al. (2017) tested a modified carbon residue from Biomass to remove SO_4^{2-} ions from an aqueous solution. It was chemically treated with different water-soluble inorganic compounds ($ZnCl_2$, $CaCl_2$, $BaCl_2$, $FeCl_3$, $FeCl_2$), and Carbon residues modified with $FeCl_3$ showed the highest removal efficiency for sulfate ions.

In another study, (Hsin et al., 2000) used synthesized metal oxide adsorbents such as γ-Al_2O_3 to investigate sulfate adsorption; the results showed that these adsorbents were significantly dependent on the electrolyte strength as they form a complex outer surface. Moreover, several studies of sulfate adsorption using metal oxides like CuO (Horányi 2004), TiO_2 (Horányi 2003a), Bi_2O_3 (Horányi 2003b), and Cr and Cr_2O_3 (Horányi 2002) were found to be dependents on the pH for oxide protonation of the layer on the surface take place.

Namasivayam and Sureshkumar (2007) studied the removal of sulfate from water and wastewater using surfactant-modified coir pith adsorbent as agricultural waste, which showed a low adsorption capacity (8.76 mg/g). Namasivayam and Sangeetha (2008) also used coconut coir pith as an adsorbent to remove sulfate and other anions from water. Results showed that raw adsorbent has an adsorption capacity of 0.06 mg/g, while modified $ZnCl_2$ activated coir pith carbon was more effective with an adsorption capacity of 4.9 mg/g. Koumaiti et al. (2011), in another study, used raw non-modified date palm seeds (RDPS) as an adsorbent for sulfate removal from wastewater. The results showed that this adsorbent exhibits a shallow adsorption capacity of 3.19 mg/g. (Sang et al., 2013) investigated poly (m-phenylenediamine)s (PmPDs) with many oxidation states to treat sulfate-containing wastewater. PmPD adsorption behavior of sulfate ions was also studied under several factors. Results showed that according to the Langmuir equation, the maximum adsorbance at solution pH of 1.75 is 108.5 mg/g. sulfate desorption efficiency is about 95%, and the accumulative adsorbance is up to 487.95 mg/g in 5 cycles.

This study obtained Kaolin clay from Mahis area- Jordan and investigated it as a potential and low-cost adsorbent for high concentration sulfate ions in a real industrial wastewater solution. Batch experiments were carried out to investigate the adsorption potential capacity of sulfate ions using modified kaolin as an adsorbent. The obtained equilibrium data were analyzed using Langmuir, Freundlich Temkin, and Dubinin-Radushkevich isotherm models. Also, the kinetic data were fitted to Pseudo-first order, Pseudo-second order, Intraparticle diffusion, and Liquid film diffusion models.

2. Materials and methods

2.1. Sulfate wastewater

The wastewater samples were collected from a local Aluminum company in Amman. The samples were settled for 24 hours then a sample was taken for analysis. This water to be treated mainly from sulfate ions will be referred to as "sulfate wastewater." The main chemical characteristics of sulfate wastewater are shown in Table 1.

Sulfate wastewateranalysis showed that sulfate ions are the main problem in this discharged wastewater with 1020 mg/L; other ions have existed like chlorides ions with 167 mg/L, silicate ions with 52 mg/L, while the total dissolved solids are 2905 mg/L, moreover, this wastewater sample is acidic, with a pH of about 5.3.

2.2. Preparation of kaolin

Kaolin clay was collected from Mahis area, Jordan. It was crushed and sieved through 5 mesh sizes (4 mm). Then it was washed and mixed with NaCl solution (0.9 M) and stirred for 4 hours. The excess NaCl was then washed and the clay was dried at 120 °C for 20 minutes. After that, it was mixed with barium chloride solution (0.5 M) and stirred for 8 hours. Finally, it was washed with ultrapure water and dried at 120 °C for 20 minutes. The $BaCl_2$ is supposed to be adsorbed to the surface of the Kaolin (Hudaib et al., 2021).

2.3. Characterization of kaolin

Both raw kaolin and modified kaolin will be characterized using Fourier Transform Infrared Spectroscopy (FTIR) instrument, model PerkinElmer, Spectrum Two L1600400, FT-IR/DTGS. The chemical composition of raw and modified kaolin used in this study was analyzed using Thermo Fisher XRF Instrument, model ARL™ SMS-Omega.

2.4. Batch adsorption technique

This adsorption study was carried out using the batch equilibration technique. A series of batch experiments were conducted by mixing different adsorbent masses ranging from 2 to 5 g with the sulfate contaminated industrial wastewater sample. Each mass was added to a 200 mL wastewater and stirred in a shaker at a speed of 230 rpm for 6 hours to ensure that equilibrium state was reached. The experiments were carried out at room temperature to be representative of environmentally relevant conditions. All experiments were performed in duplicate, and the average value was used for calculation. The pH of the industrial sulfate wastewater was 5.5. The flasks were closed to avoid any pH changes due to the exchange of gases during samples mixing. Other parameters like temperature and pH of the solution sample were kept constant. The capacity of kaolin for removing sulfate from real industrial wastewater and the effect of adsorbent dosage were investigated.

2.4.1. Sulfate measurements

The residual sulfate ions concentration in the effluent Sulfate ions product were measured using 4500-$SO4^{2-}$ E. (Turbidimetric Method) using a spectrophotometer (UV-Visible), model UV-VIS Spectrophotometer UV-1800 – Shimadzu. The measurements were carried out at a maximum wavelength (λ_{max}) of 420 nm (AWWA, APHA 1998; Sawyer et al., 2000).

2.5. Adsorption isotherms

The adsorption isotherm models are commonly applied to find out the adsorption process parameters, which provide evidence about the

Table 1. Characteristics of sulfate wastewater.

Parameter (unit)	Sulfate wastewater
SO_4^- (mg/L)	1020
Cl^- (mg/L)	167
PO_4^{-3} (mg/L)	4.9
Total hardness (mg/L)	1.9
Total dissolved solid (T.D.S) (mg/L)	2905
SiO_2^- (mg/L)	52
pH	5.3

mechanism of adsorption and the characteristics of the adsorbent. The obtained experimental equilibrium data were fitted to Langmuir, Freundlich, Temkin, and Dubinin–Radushkevich (D–R) isotherm models in this research. The values of adsorption model constants express the sorbent surface properties and affinity. The coefficient of determination of the adsorption model's linearized form is used to determine how the model fits the experimental equilibrium data.

2.5.1. Langmuir adsorption isotherm

The Langmuir model explains adsorption by a homogeneous adsorption process that takes place as a monolayer on the adsorbent's surface. The model assumes that all adsorption sites are identical and have the same adsorption energy (Doğan et al., 2000). The most widely used linearized two-parameter equation of the Langmuir model is commonly expressed as:

$$\frac{C_e}{q_e} = \frac{1}{K_a Q_m} + \frac{C_e}{Q_m} \tag{1}$$

Where C_e (mg/L) is the equilibrium concentration of cadmium ions and q_e is the amount of sulfate ions adsorbed per unit mass of adsorbent at equilibrium. Eq. (1) used in this analysis is a linearized form of the Langmuir model derived from the non-linear form. However, the transformation of data to linearized form can cause amendments of error structure, the addition of error into the independent variable, and variation of the weight placed on each data point, which leads to differences in the fitted parameter values between linear and non-linear versions (Tran et al., 2017).

2.5.2. Freundlich adsorption isotherm

The Freundlich isotherm is based on an empirical approach generated from experimental observations that can be applied for non-ideal heterogeneous adsorption. It is based on the findings that at a specific temperature, the amount of solute adsorbed at equilibrium (q_e) is linearly proportional to the concentration of solute in the solution at equilibrium, (C_e) raised to the power $1/n$. This equation may be written in the following form:

$$q_e = K_f\, C_e^{1/n} \tag{2}$$

where K_f is the Freundlich isotherm constant demonstrating the quantity of sulfate ions adsorbed onto kaolin. The higher the K_f value, the greater is the adsorption potential and significantly indicating higher adsorption capacity of the sorbent. The value of $1/n$ indicates the adsorption intensity of sulfate ions onto the modified kaolin surface. The value of $1/n$ is helpful in understanding the adsorption process at the surface. If its value is below 1, monolayer adsorption can occur, while cooperative adsorption can be assumed if its value is above 1. Eq. (2) can be appropriately linearized by taking the logarithm of both sides to get the equation:

$$\log q_e = \log K_f + \frac{1}{n} \log C_e \tag{3}$$

The degree of rationality of the experimentally measured equilibrium data to Freundlich adsorption isotherm was examined by plotting log (q_e) versus log (C_e).

2.5.3. Temkin adsorption isotherm

Temkin model isotherm is based on the assumption that there is a linear decrease in the heat of adsorption due to sorbent-adsorbate interactions. The adsorption process is explained by the fact that the binding energies are uniformly distributed up to a specific maximum value. The linearized form of Temkin isotherm is given by the relations (Hei Ing et al., 2015):

$$q_e = B_1 \ln a_t + B_1 \ln C_e \tag{4}$$

$$B_1 = RT/b_t \tag{5}$$

where b_t is a constant related to the heat of sorption (J/mol) and a_t is the Temkin isotherm constant (L/mg).

2.5.4. Dubinin-Radushkevich (D-R) isotherm

Dubinin and Radushkevich suggested an adsorption mechanism based on the distribution of Gaussian energy on a heterogeneous surface. This proposed mechanism is commonly used to understand the type of adsorption process, whether it occurs physically or chemically. Also, the Dubinin-Radushkevich model can be applied to estimate the two essential parameters: the adsorption capacity and the apparent free energy of adsorption. The linear form of the isotherm is given by the expression (Günay et al., 2007):

$$\ln q_e = \ln q_m - B \in^2 \tag{6}$$

where B ($mol^2\ KJ^{-2}$) is a constant representing the adsorption energy, q_m is the maximum adsorption capacity of the adsorbent, and $\in$ is the Polanyi adsorption potential can be evaluated from the equation:

$$\in = R\,T \ln\left(1 + \frac{1}{C_e}\right) \tag{7}$$

R is the gas constant (8.314 J $mol^{-1}\ K^{-1}$), T is the absolute temperature in K.

The mean free energy of adsorption (E) is defined as the change in free energy when transferring one mole of adsorbate to the sorbent's surface from infinity in solution. It can be calculated from the value of B, the parameter of Dubinin-Radushkevich isotherm according to the relation:

$$E = \frac{1}{\sqrt{2B}} \tag{8}$$

3. Results and discussion

3.1. Kaolin adsorbent characteristics

A mineralogical investigation of the raw and modified kaolin was carried out using XRF analysis (XRF) to determine the kaolin's chemical compositions. The elements determined in kaolin clay have been expressed as oxides in the whole sample, as shown in Table 2. According to the XRF chemical analysis, raw kaolin as an adsorbent is composed mainly of 67.35 wt% of silica and 8.62 wt% of alumina. It is clear that a large amount of hematite of about 17.48 wt% is higher than alumina. The sulfate bond's nature to iron oxides (hematite) as sulfate ion bond is known and evaluated as a strong bond. Furthermore, oxide surfaces generally are considered a very powerful adsorbent for sulfate ions (Watanabe et al., 1994). After modification, the content of SiO_2 decreased to 55.32. This could be explained to the removal of quartz impurities during the hydrothermal reaction and the fixation of about 6.73 wt% Na2O and 5.89 wt% BaO; due to the insertion of Na^+ and Ba^+ into the kaolinite structure (David et al., 2020).

Table 2. Chemical composition (XRF) of kaolin clay samples used in this study.

Compositions	Na_2O	BaO	Al_2O_3	CaO	Fe_2O_3	K_2O	MgO	SO_3	SiO_2	Loss of ignition
Raw kaolin	0.00	0.00	8.62	0.65	17.48	0.27	0.22	0.14	67.35	5.27
Modified Kaolin	6.73	5.89	8.71	1.12	17.14	0.14	0.16	0.08	55.32	4.71

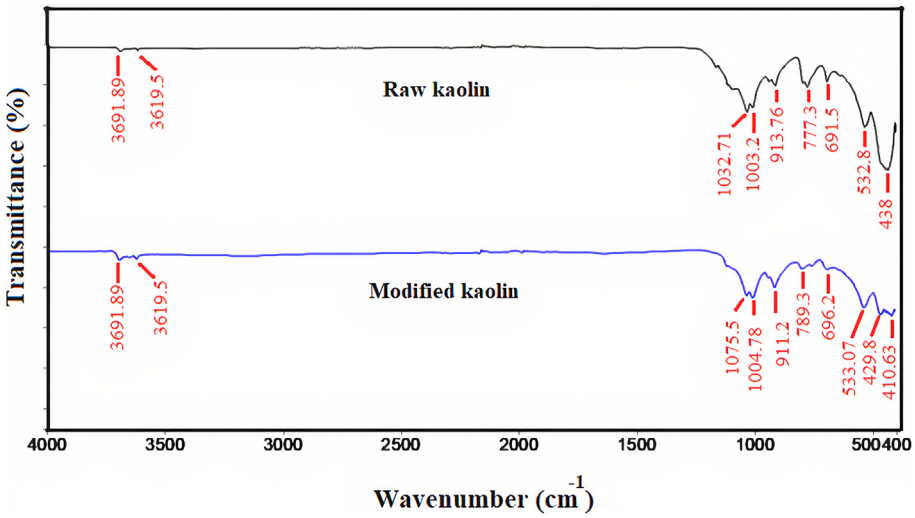

Figure 1. FTIR spectra of raw kaolin and modified Kaolin.

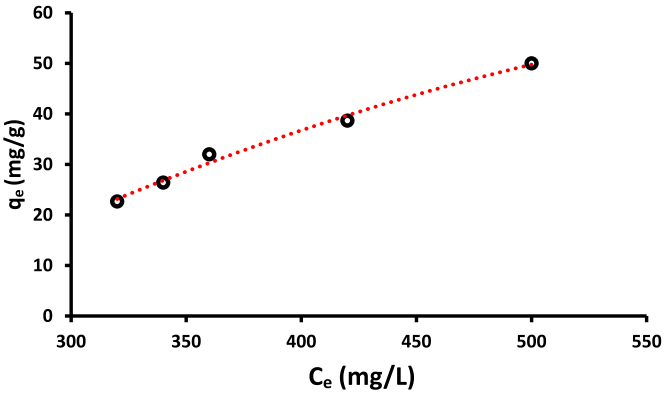

Figure 2. The experimental equilibrium data for the adsorption of sulfate ions on the modified kaolin adsorbent.

The composition of kaolin candidates is a suitable and powerful adsorbent for sulfate ions due to large oxide surfaces that can bond with sulfate ions.

3.2. FTIR analysis

The Fourier Transform Infrared Spectroscopy (FTIR) of raw kaolin, and modified kaolin are shown in Figure 1. As shown in Figure 1, in raw and modified Kaolin vibrations observed at 3691.89 cm^{-1}, and 3619.5 cm^{-1} are ascribed to the inner hydroxyl groups, located between octahedral and tetrahedral sheets (Panda et al., 2010). The vibrational bands for raw kaolin at 1032.71 cm^{-1}, 1003.78 cm^{-1}, and modified kaolin at 1075.5 cm^{-1} and 1004.78 cm^{-1} corresponded to Si–O stretching vibration.

The band at 913.76 cm^{-1} and 911.2 cm^{-1} was attributed to Si-OH or Al–Al–OH vibration. Also, peaks are shown at 777.3 cm^{-1}, and 789.3 cm-1 were referred to as Si–O–Al stretching vibration. At 691.5 cm-1 and 696.2 cm^{-1} weak absorption band was noticed for Si–O–Si bending vibration (Chai et al., 2020). A significant band was spotted for the modified kaolin at 410.63 agrees to Ba-Cl in-plane bending (Hudaib et al., 2021; Peter et al., 2018).

In conclusion, the sorption of $BaCl_2$ on Kaolin showed a negligible change in kaolin's basic structure. Hence adsorption is done by physical interaction forces can be seen mainly at 410.63 cm^{-1} (Hudaib et al., 2021, Peter et al., 2018). Moreover, the highest intensities were noticed to be slightly decreased, and the adsorption bands' position shifted significantly; this can be attributed to the bond established and may justify the feasibility of adsorption (Hudaib et al., 2021; El Mouhri et al., 2020).

3.3. Equilibrium analysis

The experimentally measured equilibrium adsorption capacity (q_e) as a function of the equilibrium concentration (C_e) for the adsorption of sulfate ions from the industrial wastewater on the modified Kaolin adsorbent at 25 °C is presented in Figure 2.

The equilibrium data presented in Figure 2 was obtained from a series of batch experiments which were conducted by mixing different masses of the adsorbent ranging from 2 to 5 g (weighed to the fourth decimal point) with the sulfate contaminated industrial wastewater sample. Each mass was added to a 200 mL wastewater and stirred in a shaker at a speed of 230 rpm for 6 hours to ensure that equilibrium state was reached. The temperature was fixed at 25 °C using the water bath of the shaker. After the stirring, the adsorbent was separated by filtration, and the remaining sulfate ions were determined. Figure 2 shows that the amount of sulfate adsorbed per unit mass of adsorbent at equilibrium, i.e., kaolin

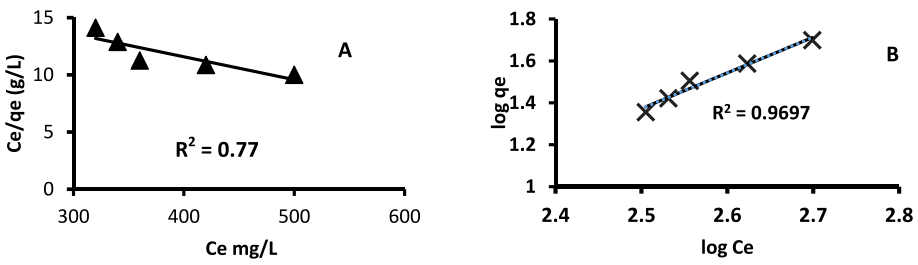

Figure 3. (A, B). Straight-line fitting of the experimental equilibrium data for the adsorption of sulfate ions from industrial wastewater onto the modified kaolin according to A- Langmuir isotherm (Equation 1) and B- Freundlich isotherm (Equation 3) at 25 °C.

Table 3. Isotherm parameters and their coefficient of determination of fitting the measured experimental equilibrium data.

Freundlich isotherm	Temkin isotherm	Dubinin-Radushkevich isotherm
$R^2 = 0.9697$	$R^2 = 0.991$	$R^2 = 0.9889$
$K_f = 0.001293$ mg $^{1-1/n}$ $L^{1/n}$ g^{-1}	$b_t = 41.46148$ J/mol	$q_m = 85.08$ mg/g
$1/n = 0.587$ & $n = 1.703$	$a_t = 0.00461$ L/mg	E = 24.87 KJ/mol

equilibrium adsorption capacity (qe) increased with increasing the equilibrium concentration (Ce) of sulfate in the wastewater and levels off at around qe= 5 mg.g^{-1}. The qe increase is due to the larger sulfate concentration gradient obtained when using a higher initial sulfate concentration (C_0).

The Langmuir equilibrium parameters Q_m (mg/g) and K_a (L/mg) represent the maximum adsorption achieved at equilibrium and the adsorbate's binding energy to the tested adsorbent, respectively. Eq. (1) was used to analyze the experimental equilibrium data obtained from the adsorption of sulfate ions from the industrial wastewater onto the modified kaolin. The linear plot of the data to this model is presented in Figure 3.

According to Langmuir isotherm Figure (3A), the plot of the experimental data shows a straight line ($R^2 = 0.77$) with a negative slope, indicating that the adsorption of sulfate ions from industrial wastewater onto the modified kaolin does not follow the assumption on which the Langmuir approach is established.

The linear Freundlich isotherm plot according to Eq. (3) is shown in Figure (3B). The Freundlich isotherm constants determined by linear regression are shown in Table 3. The coefficient of determination R^2 value of 0.9697 illustrated in Table 1 shows that the Freundlich isotherm model fits well with the experimental measurements. The obtained K_f and 1/n values from the straight line's slope and intercept Figure (3B) are 0.001293 mg $^{1-1/n}$ $L^{1/n}$ g^{-1} and 1.703, respectively. The value of 1/n is a guide for the type of adsorption (Altaher et al., 2015). If the value is less than 1, then the adsorption process is a chemical one. The value of 1/n in this adsorption process is 1.703 suggesting physical adsorption. The degree of fitting of the calculated data from the Freundlich model and the experimental measurements is depicted in Figure 5. Obviously, Figure 5 demonstrates that Freundlich isotherm reveals a rational model for the adsorption of sulfate ions on the newly prepared kaolin sorbent.

The fitting of the data to the Temkin isotherm is illustrated in Figure 4. It is clear from the linear plot of the equilibrium adsorption data presented in Figure 4 and due to the high coefficient of determination, which approaches unity ($R^2 = 0.991$), that the experimental data fit well with the Temkin model. The isotherm constants are shown in Table 3.

The adsorption energy in the Temkin model, $b_t = 41.46148$ J/mol is positive for sulfate ions adsorption on kaolin from the industrial wastewater, which indicates that the adsorption is exothermic. Comparing the calculated isotherm from the Temkin model with the experimental data presented in Figure 5 indicate that the Temkin model can be used to explain the adsorption of sulfate ions on kaolin.

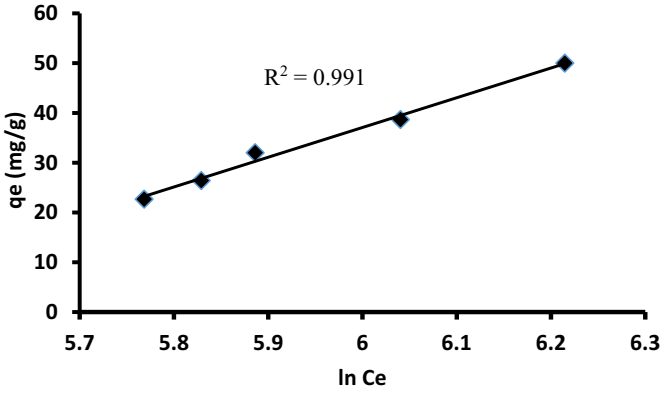

Figure 4. Fitting the obtained equilibrium adsorption data according to the linear form of the Temkin isotherm (Equation 4).

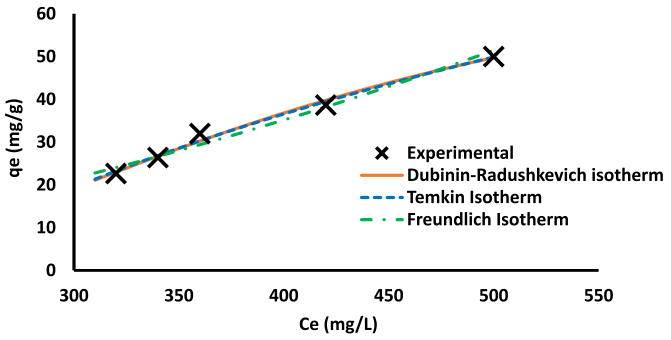

Figure 5. Comparing the measured equilibrium data with the estimated from Freundlich, Temkin, and Dubinin-Radushkevich isotherms.

The coefficients of the D-R isotherm are presented in Table 3.

A plot of ln q_e versus ϵ^2 (Figure 6) was employed to estimate the value of q_m and B. Figure 6 shows that the experimental data fulfill with a high R^2 value close to unity ($R^2 = 0.9889$) in the Dubinin-Radushkevich isotherm. The high extent of fitting the Dubinin-Radushkevich isotherm in the experimental equilibrium data can be seen clearly in Figure 5. This will be a valuable tool to estimate with confidence the maximum adsorption capacity (q_m) of kaolin for the adsorption of sulfate ions from the industrial wastewater. Also, the mean free energy value (E) will be estimated with high accuracy. These estimated parameters are presented in Table 3.

The estimated value of the maximum adsorption capacity $q_m = 85.08$ mg/g indicates that kaolin has a very high capacity to adsorb sulfate ions than other similar adsorbents, as shown in Table 4. This result indicates that the modified kaolin suits the treatment of the studied industrial wastewater, which has a very high concentration of sulfate ions.

If the mean free energy value is less than 8 KJ/mol, then the adsorption is physical. If the value is between 8 and 16 KJ/mol, the adsorption follows an ion-exchange mechanism. Values that are greater than 16 KJ/mol indicate chemical adsorption (chemisorption). The estimated value of E is very low (E = 4.87 KJ/mol). This confirms that the adsorption is a physical type.

3.4. Adsorption kinetics

The investigation of adsorption kinetics describes the rate of uptake of adsorbate as well as provides clear information about the controlling mechanism of the rate of adsorption. The adsorption kinetics of sulfate ions onto kaolin is estimated from the measured variation of adsorption capacity (qt) with time (t) shown in Figure 7. The kinetic study results

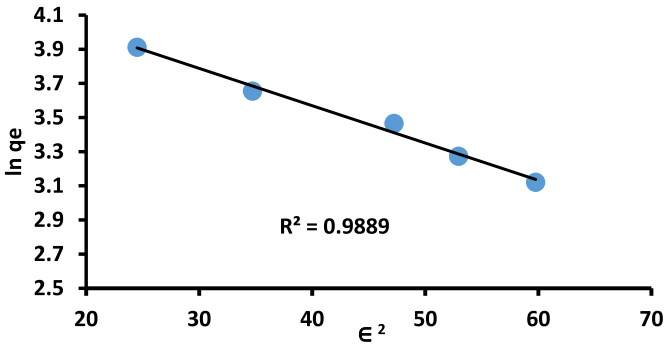

Figure 6. Linear Plot of the measured experimental data according to Dubinin-Radushkevich (Equation 7) isotherm for adsorption of sulfate ions by kaolin.

Table 4. The adsorption capacity for many different adsorbents compared with this study.

Adsorbent	Adsorption capacity (mg/g)	Reference
Halloysite and kaolinites	5.03	(Sadeghalvad et al., 2021)
Raw poorly ordered Jaroszow kaolinite (J)	1.63	(Sadeghalvad et al., 2021)
Raw well-ordered Maria III kaolinite	0.86	(Sadeghalvad et al., 2021)
Barium Modified Zeolite	62.4	(Oliveira 2007)
Barium-modified analcime	3.3	(Runtti et al., 2017)
Barium-modified acid-washed analcime	13.7	(Runtti et al., 2017)
Barium-modified zeolite	6.5	(Runtti et al., 2017)
Surfactant modified zeolite	38.02	(Chen, Liu 2014)
Surfactant modified clinoptilolite	7.49	(Vujaković et al., 2000)
limestone	23.7	(Silva et al., 2012)
Raw Quartz-Albitophire	20.27	(Sadeghalvad et al., 2016)
Modified Kaolin	85.08	Current study

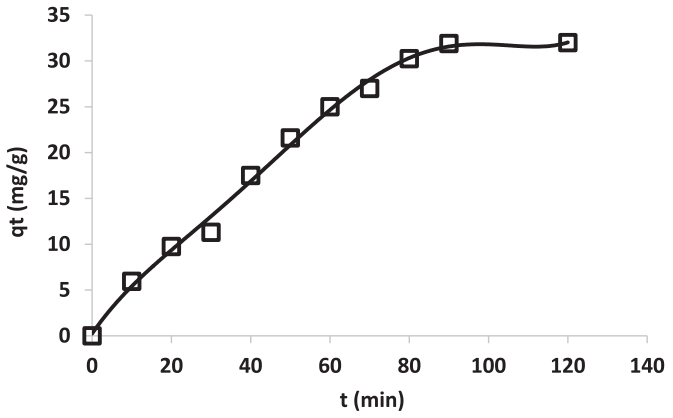

Figure 7. The measured variation of adsorption capacity with time for the adsorption of sulfate ions onto kaolin.

showed that the adsorption of sulfate ions on kaolin increased with increasing contact time and attained equilibrium at about 90 minutes, moreover, it showed that in the first hour, kaolin continued to adsorb sulfate ions, with a higher amount and velocity in the case of wastewater with respect to the sulfate solution. In the second hour, the adsorption still occurred, reaching an equilibrium at the maximum qt, 33 $mg.g^{-1}$.

In this study, the Pseudo-first order model, Pseudo-second order model, Intra-particle diffusion model, and Liquid film diffusion model are applied to analyze adsorption kinetics using the experimental data presented in Figure 7.

Pseudo–first-order kinetic model is based on the hypothesis that the rate of change of solute sorption is directly proportional with time to the difference between the saturation concentration of sorbent and the amount of sorbent uptake with time. It is frequently detected that kinetics follows the pseudo-first-order rate equation when adsorption is controlled by diffusion through the interface. The pseudo-first-order kinetics of adsorption can be described by Eq. (9) (Chiou and Li 2003).

$$log(q_e - q_t) = log(q_e) - \left(\frac{k_1}{2.303}\right) t \quad (9)$$

where q_e and q_t (mg/g) are the amounts of sulfate ions adsorbed on kaolin at equilibrium and at time t, respectively, and k_1 is the pseudo-first-order rate constant (min^{-1}). The results of the linear plot of $log(q_e - q_t)$ versus t according to Eq. (9) is shown in Table 2. The rate constant, k_1 and coefficient of determination, R^2 are 0.032703 min^{-1} and 0.9066, respectively. Figure 7 shows the extent to which that pseudo-first-order model fits our experimental kinetic data. Obviously, our experimental data follows this model, indicating that diffusion through the interface is an important mechanism.

The pseudo-second-order kinetic model is based on the assumption that the rate-limiting step is chemical sorption or chemisorption. The linear equation of the pseudo-second-order adsorption kinetic rate is given by Eq. (10) (Ho 2006):

$$\frac{t}{q_t} = \frac{1}{k_2\, q_e^2} + \frac{1}{q_e}\, t \quad (10)$$

where k_2 is the pseudo-second-order rate constant in (g mg^{-1} min^{-1}). The results obtained from the linear plot of t/q_t Versus t according to Eq. (10) are presented in Table 5. The determined rate constant, k_2 and coefficient of determination, R^2 are 0.0678 g mg^{-1} min^{-1} and 0.8011, respectively. By inspecting Figure 8, it is clear that the pseudo-second-order kinetic model poorly fits the experimental data as the Pseudo-first order designating that the rate-limiting step may be more physical than chemical adsorption (Ngah et al., 2005). Consequently, the pseudo-first-order model could better describe sulfate ions' adsorption on kaolin than the pseudo-second-order model.

In a stirred batch adsorption process, the transport of sulfate ions from the bulk of the wastewater into the kaolin is mainly governed by an intraparticle diffusion process, which is often the rate-limiting step in many adsorption processes (Santhi and Manonmani 2010). The linear equation describing the intraparticle diffusion process as shown in Eq. (11):

$$q_t = k_{id} t^{0.5} + C \quad (11)$$

where k_{id} (mg/g.$min^{-0.5}$) is the rate constant for the intraparticle diffusion model, and C represents the boundary layer's thickness. The boundary layer effect is greater for the larger C value. If the intraparticle diffusion is the rate-determining step, then the data must fit the intraparticle diffusion model. The results presented in Table 5 show a high coefficient of determination (R^2 = 0.9531), displaying that the intraparticle diffusion process can describe our experimental measurement to a high degree. Consequently, intraparticle diffusion is involved in the adsorption process and might be a limiting mechanism. The high degree of agreement between the intraparticle diffusion model and our experimental data is seen in Figure 8.

The liquid film diffusion model can be applied to test if the diffusion process controls the adsorption of sulfate ions by kaolin and if the solute molecules' rate from the liquid phase to the solid phase through the boundary layer controls the sulfate ions/kaolin adsorption system. Eq. (12) illustrates the liquid film diffusion model:

Table 5. Pseudo-first order, Pseudo-second order, Intraparticle diffusion, and liquid film diffusion model parameters for sulfate ions adsorption onto kaolin.

Pseudo-first-order	pseudo second-order	Intraparticle diffusion	Liquid film diffusion
R^2 (Eq. 9) = 0.9066	R^2 (Eq. 10) = 0.8011	R^2 = 0.9531	R^2 = 0.75
k_1 = 0.032703 min^{-1}	k_2 = 0.0678 g mg^{-1} min^{-1}	k_{id} = 3.934 mg/g.$min^{-0.5}$	k_d = 0.0557 min^{-1}

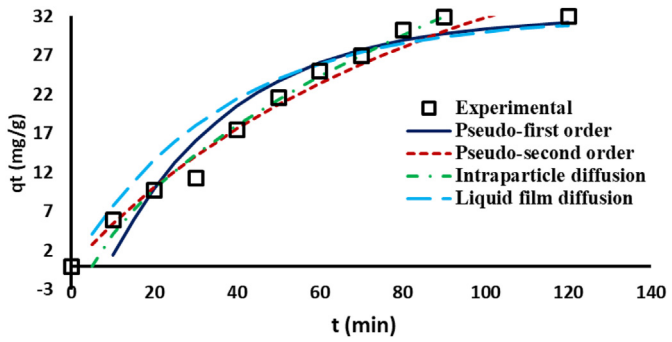

Figure 8. Comparison of the measured and predicted kinetics from Pseudo-first order, Pseudo-second order, Intraparticle diffusion, and Liquid film diffusion kinetic models for sulfate adsorption ions onto kaolin.

$$\ln\left(1-\frac{q_t}{q_e}\right) = -k_d\, t \tag{12}$$

Where k_d is the diffusion rate constant (min^{-1}). The linear plot results of our experimental data according to Eq. (12) are presented in Table 5.

The Liquid film diffusion model poorly fits the experimental data (R^2 = 0.75), indicating that the liquid diffusion step is not the rate-controlling step. This can be predicted in Figure 8.

4. Conclusions

In this study, Jordanian kaolin was successfully modified and used as a potential adsorbent for the treatment of industrial high-sulfate wastewater effluents. The study's result proved that this innovative natural sorbent is effective in the treatment of industrial wastewater effluents. The adsorption capacity was found to be 85.08 mg/g indicating that kaolin has a high capacity to adsorb sulfate ions at studied parameters. The equilibrium data were analyzed using four adsorption models, Langmuir, Freundlich, Temkin, and Dubinin-Radushkevich isotherm models. Freundlich adsorption isotherm was found to fit the experimental data to a high degree. The obtained K_f and 1/n values are 0.001293 mg $^{1-1/n}$ L $^{1/n}$ g^{-1} and 1.703, respectively, suggesting physical adsorption. The analysis indicated that the experimental data also fit well with the Temkin and Dubinin-Radushkevich isotherm models. The estimated value of the mean free energy (4.87 kJ/mol) is very low, confirming physical type adsorption. Experimental data were correlated perfectly to the pseudo-first-order and intraparticle diffusion models, which justifies that the adsorption process has a physical nature. The previous results show that modified Jordanian kaolin is a safe, effective natural adsorbent for sulfate-contaminated industrial wastewater.

Declarations

Author contribution statement

Dr. Banan Hudaib: Conceived and designed the experiments; Performed the experiments; Analyzed and interpreted the data; Contributed reagents, materials, analysis tools or data; Wrote the paper.

Funding statement

This research did not receive any specific grant from funding agencies in the public, commercial, or not-for-profit sectors.

Data availability statement

Data included in article/supplementary material/referenced in article.

Declaration of interests statement

The authors declare no conflict of interest.

Additional information

No additional information is available for this paper.

References

Akoh, F., Bouchoum, H., Bouchti, M El, Cherkaoui, O., Jada, A., Tahiri, M., 2020. Sulfate removal from aqueous solutions using esterified wool fibers: isotherms, kinetic and thermodynamic studies. Desalin. Water Treat. 194, 417–428.

Altaher, H., Alghamdi, A., Omar, W., 2015. Innovative biosorbent for the removal of cadmium ions from wastewater. Environ. Eng. Manag. J. 14, 793–800.

Al-Zoubi, H., Hilal, N., Darwish, N.A., Mohammad, A.W., 2007. Rejection and modelling of sulphate and potassium salts by nanofiltration membranes: neural network and Spiegler–Kedem model. Desalination 206 (1), 42–60.

Al-Zoubi, H., Zubair, M., Manzar, M.S., Manda, A.A., Blaisi, N.I., Qureshi, A., et al., 2020. Comparative adsorption of anionic dyes (eriochrome black T and Congo red) comparative adsorption of anionic dyes (eriochrome black T and Congo red) onto jojoba residues : isotherm , kinetics and thermodynamic studies. Arabian J. Sci. Eng. 45, 7275–7287.

Amaral Filho, J., Azevedo, A., Etchepare, R., Rubio, J., 2016. Removal of sulfate ions by dissolved air flotation (DAF) following precipitation and flocculation. Int. J. Miner. Process. 149, 1–8.

AWWA, WEF, APHA, 1998. Standard Methods for the Examination of Water and Wastewater.

Cao, W., Dang, Z., Zhou, X.-Q., Yi, X.-Y., Zhu, N., Lu, G., 2011. Removal of sulphate from aqueous solution using modified rice straw: preparation, characterization and adsorption performance. Carbohydr. Polym. 85, 571–577.

Chai, J.-B., Au, P.-I., Mujawar, M., Khalid, M., Ng, W., Jagadish, P., et al., 2020. Adsorption of heavy metal from industrial wastewater onto low-cost Malaysian kaolin clay–based adsorbent. Environ. Sci. Pollut. Res. 27.

Chen, W., Liu, H., 2014. Adsorption of sulfate in aqueous solutions by organo-nano-clay: adsorption equilibrium and kinetic studies. J. Cent South Univ. 21, 1974–1981.

Chiou, M.S., Li, H.Y., 2003. Adsorption behavior of reactive dye in aqueous solution on chemical cross-linked chitosan beads. Chemosphere 50 (8), 1095–1105.

David, Moses Kolade, Chris Okoro, Uchechukwu, Godfrey Akpomie, Kovo, Okey, Christian, Olumayowa Oluwasola, Henry, 2020. Thermal and hydrothermal alkaline modification of kaolin for the adsorptive removal of lead(II) ions from aqueous solution. SN Appl. Sci. 2 (6), 1–13.

Dhayabaran, N.K., Narayana, A., Arivazhagan, M., 2017. Removal of high concentration of sulfate from pigment industry effluent by chemical precipitation using barium chloride: RSM and ANN modeling approach. J. Environ. Manag. 206, 69–76.

Diab, A., Zoromba, M., Hussien, M., Sherif, M., 2015. Comparison between adsorption of copper ions by kaolinite and kaolinite composite. J. Soil Water Sci. 2, 1–8.

Doğan, M., Alkan, M., Onganer, Y., 2000. Adsorption of methylene blue from aqueous solution onto perlite. Water Air Soil Pollut. 120, 229–248.

El Mouhri, G., Merzouki, M., Hajar, B., Miyah, Y., Amakdouf, H., El Mountassir, R., et al., 2020. Continuous adsorption modeling and fixed bed column studies: adsorption of tannery wastewater pollutants using beach sand. J. Chem. 2020, 1–9.

Günay, A., Arslankaya, E., Tosun, İ., 2007. Lead removal from aqueous solution by natural and pretreated clinoptilolite: adsorption equilibrium and kinetics. J. Hazard Mater. 146 (1), 362–371.

Hei Ing, C., Priyantha, N., Lim, L., 2015. Effective adsorption of toxic brilliant green from aqueous solution using peat of Brunei Darussalam: isotherms, thermodynamics, kinetics and regeneration studies. RSC Adv. 5.

Ho, Y.-S., 2006. Second-order kinetic model for the sorption of cadmium onto tree fern: a comparison of linear and non-linear methods. Water Res. 40 (1), 119–125.

Horányi, G., 2004. Comparison of the specific adsorption of sulfate (HSO4−) ions on Cr and Cr_2O_3. J. Solid State Electrochem. 8 (4), 215–217.

Horányi, G., 2003a. Investigation of the specific adsorption of sulfate ions on powdered TiO_2. J. Colloid Interface Sci. 261 (2), 580–583.

Horányi, G., 2003b. Radiotracer study of the adsorption of sulfate ions at a Bi_2O_3 powder/electrolyte solution interface. J. Solid State Electrochem. 7 (5), 309–312.

Horányi, G., 2002. Specific adsorption of anions preceding the dissolution of CuO in acidic solution. J. Solid State Electrochem. 6 (7), 463–467.

Hsin, wu, Lo, S.-L., Lin, C.-F., 2000. Competitive adsorption of molybdate, chromate, sulfate, selenate, and selenite on γ-Al2O3. Colloid. Surf. A-Physicochem. Eng. Asp - Colloid Surf A. 166, 251–259.

Hudaib, B., Al-shawabkeh, A.F., Omar, W., Al-zoubi, H., Abu-zurayk, R., 2021. Removal of high-concentration sulfate ions from industrial wastewater using low-cost modified Jordanian kaolin. J. Chem 27503, 1–8.

Koumaiti, S., Riahi, K., Ounaies, F., Thayer, B Ben, 2011. Kinetic modelling of liquid-phase adsorption of sulfate onto raw date palm seeds. J. Environ. Sci. Eng. 5 (12).

Ministry of Water and Irrigation, 2009. Water-Natural Water. http://www.jsmo.gov.jo/en/EServices/Standards/Pages/StdLists.aspx?ics=1306020.

Moret, A., Rubio, J., 2003. Sulphate and molybdate ions uptake by chitin-based shrimp shells. Miner. Eng. 16 (8), 715–722.

Mulinari, D.R., da Silva, M.L.C.P., 2008. Adsorption of sulphate ions by modification of sugarcane bagasse cellulose. Carbohydr. Polym. 74 (3), 617–620.

Mustapha, S., Ndamitso, M.M., Abdulkareem, A.S., Tijani, J.O., Mohammed, A.K., Shuaib, D.T., 2019. Potential of using kaolin as a natural adsorbent for the removal of pollutants from tannery wastewater. Heliyon 5 (11), 02923.
Namasivayam, C., Sangeetha, D., 2008. Application of coconut coir pith for the removal of sulfate and other anions from water. Desalination 219 (1), 1–13.
Namasivayam, C., Sureshkumar, M., 2007. Removal of sulfate from water and wastewater by surfactant modified coir pith, an agricultural solid' waste' by adsorption methodology. J. Environ. Eng, Manag. 17.
Ngah, W.S.W., Ab Ghani, S., Kamari, A., 2005. Adsorption behaviour of Fe(II) and Fe(III) ions in aqueous solution on chitosan and cross-linked chitosan beads. Bioresour. Technol. 96 (4), 443–450.
Oliveira, C.R., Rubio, J., 2007. New basis for adsorption of ionic pollutants onto modified zeolites. Miner. Eng. 20 (6), 552–558.
Panda, A.K., Mishra, B.G., Mishra, D.K., Singh, R.K., 2010. Effect of sulphuric acid treatment on the physico-chemical characteristics of kaolin clay. Colloids Surf. A Physicochem. Eng. Asp 363 (1), 98–104.
Peter, E., Dabulo1, A., Thillainayagam, G., 2018. Growth and characterization of barium chloride dihydrate crystal. Int. J. Sci. Res. 2 (1), 19–24.
Rodrigues, C., Follmann, H., Núñez-Gómez, D., Nagel-Hassemer, M.E., Lapolli, F., Lobo-Recio, M., 2020. Sulfate removal from mine-impacted water by electrocoagulation: statistical study, factorial design, and kinetics. Environ. Sci. Pollut. Res. 27, 39572–39583.
Runtti, H., Tynjälä, P., Tuomikoski, S., Kangas, T., Hu, T., Rämö, J., et al., 2017. Utilisation of barium-modified analcime in sulphate removal: isotherms, kinetics and thermodynamics studies. J. Water Process Eng. 16, 319–328.
Santhi, T., Manonmani, S., 2010. Kinetics and isotherm studies on cationic dyes adsorption onto annona squmosa seed activated carbon. Int. J. Eng. Sci. Technol. 2.
Sadeghalvad, B., Azadmehr, A., Hezarkhani, A., 2016. Enhancing adsorptive removal of sulfate by metal layered double hydroxide functionalized Quartz-Albitophire iron ore waste: preparation, characterization and properties. RSC Adv. 6, 67630–67642.
Sadeghalvad, B., Azadmehr, A., Hezarkhani, A., 2017. Sulfate decontamination from groundwater by metal layered double hydroxides functionalized high phosphorus iron ore waste as a new green adsorbent: experimental and modeling. Ecol. Eng. 106, 219–230.
Sadeghalvad, B., Khorshidi, N., Azadmehr, A., Sillanpää, M., 2021. Sorption, mechanism, and behavior of sulfate on various adsorbents: a critical review. Chemosphere 263.
Saidan, M.N., Al-Addous, M., Al-Weshah, R.A., Obada, I., Alkasrawi, M., Barbana, N., 2020. Wastewater reclamation in major Jordanian industries: a viable component of a circular economy. Water 12 (5).
Sang, P., Wang, Y., Zhang, L., Chail, L., Wang, H., 2013. Effective adsorption of sulfate ions with poly(m-phenylenediamine) in aqueous solution and its adsorption mechanism. Trans. Nonferrous Met. Soc. China 23 (1), 243–252.
Sawyer, C.N., McCarty, P.L., Parkin, G.F., 2000. Chemistry for Environmental Engineering, fourth ed. McGraw-Hill, Inc., New York.
Shaban, M., Sayed, M., Shahien, M., Abukhadra M, R., Ahmed, Z., 2018. Adsorption behavior of inorganic- and organic-modified kaolinite for Congo red dye from water, kinetic modeling, and equilibrium studies. J. Sol. Gel Sci. Technol. 87 (3).
Silva, A.M., Lima, R.M.F., Leão, V.A., 2012. Mine water treatment with limestone for sulfate removal. J. Hazard Mater. 221–222, 45–55.
Tang, W., He, D., Zhang, C., Waite, T.D., 2017. Optimization of sulfate removal from brackish water by membrane capacitive deionization (MCDI). Water Res. 121 (Mcdi), 302–310.
Tejada-Tovar, C., Villabona-Ortíz, Á., Gonzalez-Delgado, A.D., Herrera, A., Viera De la Voz, A., 2021. Efficient sulfate adsorption on modified adsorbents prepared from Zea mays stems. Appl. Sci. 11 (4), 1596.
Tran, H.N., You, S.-J., Hosseini-Bandegharaei, A., Chao, H.-P., 2017. Mistakes and inconsistencies regarding adsorption of contaminants from aqueous solutions: a critical review. Water Res. 120, 88–116.
Vujaković, A.D., Tomašević-Čanović, M.R., Daković, A.S., Dondur, V.T., 2000. The adsorption of sulphate, hydrogenchromate and dihydrogenphosphate anions on surfactant-modified clinoptilolite. Appl. Clay Sci. 17 (5), 265–277.
Watanabe, H., Gutleben, C.D., Seto, J., 1994. Sulfate ions on the surface of maghemite and hematite. Solid State Ionics 69 (1), 29–35.